Weierstraß-Institut
für Angewandte Analysis und Stochastik

im Forschungsverbund Berlin e.V.

Preprint ISSN 0946 – 8633

Numerical algorithms for Schrödinger equation with artificial boundary conditions

Raimondas Čiegis[1], Inga Laukaitytė[1], Mindaugas Radziunas[2]

submitted: 30 September 2009

[1] Vilnius Gediminas Technical University
Saulėtekio al. 11
LT-10223 Vilnius
Lithuania
E-Mail: rc@fm.vgtu.lt
Inga.Laukaityte@fm.vgtu.lt

[2] Weierstraß-Institut für
Angewandte Analysis und Stochastik
Mohrenstrasse 39
D – 10117 Berlin
Germany
E-Mail: radziuna@wias-berlin.de

No. 1446
Berlin 2009

2000 *Mathematics Subject Classification.* 65M06, 65M12, 35Q40.

Key words and phrases. Finite difference method, Schrödinger problem, absorbing boundary conditions, transparent boundary conditions, numerical experiments .

Supported by the DFG Research Center MATHEON "Mathematics for key technologies".

Edited by
Weierstraß-Institut für Angewandte Analysis und Stochastik (WIAS)
Mohrenstraße 39
10117 Berlin
Germany

Fax: + 49 30 2044975
E-Mail: preprint@wias-berlin.de
World Wide Web: http://www.wias-berlin.de/

Abstract. We consider a one-dimensional linear Schrödinger problem defined on an infinite domain and approximated by the Crank-Nicolson type finite difference scheme. To solve this problem numerically we restrict the computational domain by introducing the reflective, absorbing or transparent artificial boundary conditions. We investigate the conservativity of the discrete scheme with respect to the mass and energy of the solution. Results of computational experiments are presented and the efficiency of different artificial boundary conditions is discussed.

1. Introduction

Schrödinger type mathematical models are used in many areas of physical and technological interest, e.g. in electromagnetic wave propagation, in seismic migration and in semiconductor devices [1].

Depending on the considered real life application we frequently need to solve Schrödinger type equations in infinite or, at least, quite large spatial domains using rather fine numerical mesh [2, 3]. In these cases due to computational restrictions (CPU time and memory resources of the computer), one has to restrict the computational domain and to solve the problem only in the region of interest or a slightly larger domain.

Then the main challenge is to introduce special artificial boundary conditions which enable us to simulate accurately the asymptotical behavior of the solution and do not induce numerical reflections at the boundaries. These boundary conditions must give a well posed problem and discrete approximations of the new boundary value problem should be constructed, which are stable under non-restrictive conditions on space and time steps of the discrete grids.

There are many papers devoted to formulation and numerical analysis of absorbing boundary conditions (ABC) for solving Schrödinger equation. In [4] the first and second order ABC are proposed and approximated by the implicit finite difference scheme. Stability and convergence analysis of discrete approximations of ABC on staggered grids are given in [5]. Design of efficient discrete high-order ABC for wave and Schrödinger type problems is considered in [6, 7].

In [2] it is proposed to define additional layers near the boundary of the domain, where an artificial material has a property of strong absorption. Thus, instead of absorbing boundary conditions, a special thin absorbing layer is used, which should prevent introduction of numerical reflections from the boundaries of the restricted computational domain.

For simple wave transport models it is possible to construct such boundary conditions on the boundary of computational domain which give the exact solution of the whole-space problem. These boundary conditions are called *transparent boundary conditions* (TBC). Transparent boundary conditions were investigated for Schrödinger type equations in [8, 9], for underwater acoustics in [10, 9], for hyperbolic transport equations in [11]. A review on transparent and artificial BCs for linear and nonlinear Schrödinger equations is given in [12].

Our paper investigates the performance of numerical schemes for 1-dimensional linear Schrödinger equations with different artificial boundary conditions. By comparing the numerical solutions with the initially known solution of the corresponding problem in infinite domain we draw several conclusions about effectiveness of the considered boundary conditions. The paper is organized as follows. In Section 2 we give a full description of the mathematical problem and define three types of artificial BC. The main conservation properties of the solution are proved. Section 3 is devoted to numerical discretization of the given problem. The main attention is given to the efficient discretization of absorbing and transparent boundary conditions. It is proved that the proposed difference schemes conserve the discrete analogous of the mass and the energy. Results of computational experiments are presented and discussed. Some final conclusions are done in Section 4.

2. Problem formulation

We consider a case of the pure initial value problem for the one dimensional Schrödinger equation:

$$\begin{aligned} &\frac{\partial \tilde{u}}{\partial t} + iD_f \frac{\partial^2 \tilde{u}}{\partial x^2} - iV(x)\tilde{u} = 0, \quad x \in \mathcal{R},\ t > 0, \\ &\tilde{u}(x,0) = u_0(x), \quad x \in \mathcal{R}, \end{aligned} \tag{2.1}$$

here a real function $V(x)$ defines a given potential. We assume that the initial data $u_0(x)$ is supported only on some finite domain.

For many applications, due to computational requirements, the domain of interest is restricted to a bounded interval $\bar{\Omega}_{\tilde{X}} = [-\tilde{X}, \tilde{X}]$ with a specified (and not very large) $\tilde{X}$. Following [7], our goal is to formulate artificial boundary conditions and/or real positive sink term $\alpha = \alpha(x)$ on the extended interval $\Omega_X = (-X, X)$ with $X > \tilde{X}$ as close to $\tilde{X}$ as possible, such that the solution $u(x,t)$ of problem

$$\frac{\partial u}{\partial t} + iD_f \frac{\partial^2 u}{\partial x^2} + \big(\alpha(x) - iV(x)\big)u = 0, \quad x \in \Omega_X,\ t > 0, \tag{2.2}$$

$$\begin{aligned} &u(x,0) = u_0(x), \quad x \in \bar{\Omega}_X, \\ &F_L u(-X,t) = 0, \quad F_R u(X,t) = 0, \quad t > 0 \end{aligned} \tag{2.3}$$

is close to the exact solution of (2.1), e.g. it satisfies the estimate

$$\int_0^T \int_{-\tilde{X}}^{\tilde{X}} |\tilde{u}(x,t) - u(x,t)|^2 \, dx dt \le \varepsilon^2. \tag{2.4}$$

It turns out that for classical boundary conditions all known algorithms that guarantee the fulfilment of the condition given above are computationally very expensive. Thus in practice, we minimize the amplitudes of reflective waves and try to avoid the numerical introduction of oscillations of solutions. The BC operators $F_{L,R}$ should be local operators in space and time and define a well-posed problem for the Schrödinger equation.

If possible, the introduction of artificial boundary conditions should not destroy the conservation or dissipation relations for the mass M and energy E of the solution defined in the considered finite domain Ω_X:

$$M(t) = \|u(\cdot,t)\|^2\,, \quad E(t) = D_f \|\frac{\partial u}{\partial x}(\cdot,t)\|^2 + \int_{-X}^{X} V(x)\,|u(x,t)|^2\,dx,$$

where (u,v) and $\|u\|$

$$(u,v) = \int_{-X}^{X} u(x) v^*(x)\,dx, \quad \|u\| = \sqrt{(u,u)}$$

denote the inner product and norm of functions u, v in the $L_2(\Omega_X)$ space, respectively. It is well known that for non-dissipative problems these quantities are conserved.

2.1. **Reflective boundary conditions.** The most simple way to select the required boundary conditions is to solve problem (2.2) in a sufficiently large domain with the following reflective boundary conditions:

$$u(-X,t) = 0, \quad u(X,t) = 0, \quad t > 0. \tag{2.5}$$

These boundary conditions should be placed at a large distance from the relevant interior domain in such a way that the reflected waves would not perturb the exact solution. We note that this approach can lead to a very costly numerical algorithm. In order to reduce the length of the computational domain a real positive sink function $\alpha(x)$ can be introduced in the extended space domain (see [13], where this technique was applied for wave propagation problems).

Lemma 2.1. *If $\alpha(x) \geq 0$ and $u(x,t)$ is the solution of problem (2.2), (2.3), (2.5), then the total mass of the solution is not increased in time:*

$$M(t) \equiv \|u(\cdot,t)\|^2 \leq \|u_0\|^2 \equiv M(0). \tag{2.6}$$

If $\alpha(x) \equiv 0$ (i.e. the potential function is real valued), then the total mass and the energy $E(t)$ of the solution are conserved in time:

$$\|u(\cdot,t)\|^2 = \|u_0\|^2, \quad E(t) = E(0). \tag{2.7}$$

Proof. Computing the inner product of equation (2.2) with $u(x,t)$, integrating by parts the diffraction operator and taking the real part of the obtained equality we get the equation

$$\frac{d}{dt}\|u(\cdot,t)\|^2 + 2\int_{-X}^{X} \alpha(x)\,|u(x,t)|^2\,dx = 0.$$

Taking into account that $\alpha \geq 0$, the proof of (2.6) follows trivially. In the case of $\alpha \equiv 0$, a direct consequence is that the total mass of the solution is conserved $M(t) = M(0)$.

In order to prove the second equality in (2.7) we compute the inner product of equation (2.2) with $\frac{\partial}{\partial t}u(x,t)$, integrate by parts the diffraction operator, take the imaginary part of the the obtained equality and get

$$\frac{\partial}{\partial t}\Big(D_f\Big\|\frac{\partial u}{\partial x}(\cdot,t)\Big\|^2 + \int_{-X}^{X} V(x)\,|u(x,t)|^2\,dx\Big) = 2\int_{-X}^{X} \alpha(x)\,\mathrm{Im}\Big(u\frac{\partial u^*}{\partial t}\Big)\,dx. \tag{2.8}$$

The absorption term disturbs the conservativity of the energy $E(t)$. If $\alpha \equiv 0$, then we get the energy conservation law $\frac{d}{dt}E(t) = 0$. □

Since we consider a 1-dimensional problem, the equalities (2.7) imply the following estimates of the solution in the maximum norm $\|u(\cdot,t)\|_\infty = \max_{-X \le x \le X} |u(x,t)|$:

Lemma 2.2. *Let $u(x,t)$ be the solution of problem (2.2), (2.3), (2.5). If $\alpha(x) \equiv 0$ and $V(x) \ge -qD_f\pi^2/4X^2$ for $0 \le q < 1$ then $u(x,t)$ is bounded unconditionally in the maximum norm*

$$\|u(\cdot,t)\|_\infty \le \sqrt{XE(0)/2D_f(1-q)}. \tag{2.9}$$

Proof. We apply the following Sobolev imbedding inequalities [14, 15]:

$$\|u(\cdot,t)\|_\infty \le \frac{\sqrt{2X}}{2} \left\| \frac{\partial u}{\partial x}(\cdot,t) \right\|, \quad \|u(\cdot,t)\| \le \frac{2X}{\pi} \left\| \frac{\partial u}{\partial x}(\cdot,t) \right\|. \tag{2.10}$$

The statement of the lemma follows immediately from the energy conservation law (2.6)

$$E(0) = D_f \left\| \frac{\partial u}{\partial x}(\cdot,t) \right\|^2 + \int_{-X}^{X} V(x)\,|u(x,t)|^2\,dx \ge D_f(1-q) \left\| \frac{\partial u}{\partial x}(\cdot,t) \right\|^2$$
$$\ge \frac{2D_f(1-q)}{X} \|u(\cdot,t)\|_\infty^2.$$

□

In [16] the discrete invariants of the solution were used to prove the convergence of the discrete solution for the nonlinear Schrödinger problem with cubic and quintic terms.

2.2. **Absorbing boundary conditions.** A convenient way to transform a large computational domain Ω to a smaller subdomain is to use absorbing boundary conditions. The main idea is to mimic the movement of a simple wave traveling to the right or left directions (see, [5]).

Let us consider left/right moving single waves $u(x,t) = e^{i(\omega t \pm kx)}$, where $\omega(k)$ denotes the wave frequency and k is the wave number. Parameters ω and k are connected by the dispersion relation, which follows from the Schrödinger equation (2.2):

$$\omega(k) = D_f k^2 + V.$$

The group velocity of the wave is defined as $v := \frac{\partial \omega}{\partial k} = 2D_f k$. Next we use the relation $\frac{\partial u}{\partial x} = \pm iku$ (for left/right moving waves, respectively), and get the following absorbing boundary conditions

$$-iD_f \frac{\partial u}{\partial x}\big(-X,t\big) = \gamma u(-X,t), \quad iD_f \frac{\partial u}{\partial x}\big(X,t\big) = \gamma u(X,t), \tag{2.11}$$

where $\gamma = v/2$. For such absorbing BCs simple waves traveling with a group velocity v are absorbed completely. However, in applications, waves are composed of many components moving with different velocities. Our goal is to investigate the efficiency of absorbing boundary conditions in a general case, and to determine optimal values of parameter γ in (2.11).

Lemma 2.3. *Let $\alpha(x) \equiv 0$ and $u(x,t)$ is the solution of problem (2.2), (2.3), (2.11), then the total mass of the solution is not increased in time:*

$$M(t) \equiv \|u(\cdot,t)\|^2 \le \|u_0\|^2 \equiv M(0). \tag{2.12}$$

The energy $E(t)$ of the solution satisfies the following conservation equation

$$\begin{aligned} \frac{\partial}{\partial t}\Big(D_f \left\|\frac{\partial u}{\partial x}(\cdot,t)\right\|^2 + \int_{-X}^{X} V(x)\,|u(x,t)|^2\,dx\Big) \\ = 2\gamma\Big(\mathrm{Im}\Big(u\frac{\partial u^*}{\partial t}\big(-X,t\big)\Big) + \mathrm{Im}\Big(u\frac{\partial u^*}{\partial t}\big(X,t\big)\Big)\Big). \end{aligned} \tag{2.13}$$

Proof. Computing the inner product of equation (2.2) with $u(x,t)$, integrating by parts the diffraction operator, using boundary conditions (2.11) and taking the real part of the obtained equality we get the equation

$$\frac{d}{dt}\|u(\cdot,t)\|^2 + 2\gamma\left(|u(-X,t)|^2 + |u(X,t)|^2\right) = 0.$$

Taking into account that $\gamma > 0$, the proof of (2.12) follows trivially.

In order to prove (2.13), we compute the inner product of equation (2.2) with $\frac{\partial}{\partial t}u(x,t)$, integrate by parts the diffraction operator, use the absorbing boundary conditions and take the imaginary part of the the obtained equality. In this case the absorption boundary conditions disturb the conservativity of the energy $E(t)$. □

In general, waves are composed of more than one component with different group velocities. Therefore in [4] a generalization of absorbing BCs (2.11) is proposed (see also [5], where discrete approximations of these BCs are considered):

$$\prod_{j=1}^{p}\Big(\pm iD_f\frac{\partial}{\partial x} - \gamma_j\Big)u\Big|_{x=\pm X} = 0. \tag{2.14}$$

Let us consider the case $p = 2$ and take $\alpha \equiv 0$. In this case (2.14) and (2.2) imply:

$$\pm iD_f\frac{\partial u}{\partial x}\big(\pm X,t\big) = \frac{1}{\gamma_1+\gamma_2}\Big(\gamma_1\gamma_2 u - D_f V u - iD_f\frac{\partial u}{\partial t}\Big)\Big|_{x=\pm X}. \tag{2.15}$$

Let us check, if inequality (2.12) is valid for Schrödinger problem (2.2), (2.3) with BCs (2.15). For most applications we can assume that $V(\pm X) = 0$. Computing the inner product of equation (2.2) with $u(x,t)$, integrating by parts the diffraction operator, using boundary conditions (2.15) and taking the real part of the obtained equality we get the equation

$$\frac{d}{dt}\|u(\cdot,t)\|^2 + \frac{2\gamma_1\gamma_2}{\gamma_1+\gamma_2}\left(|u(-X,t)|^2 + |u(X,t)|^2\right)$$
$$= 2\frac{D_f}{\gamma_1+\gamma_2}\left(\mathrm{Im}\left(u\frac{\partial u^*}{\partial t}(-X,t)\right) + \mathrm{Im}\left(u\frac{\partial u^*}{\partial t}(X,t)\right)\right).$$

It follows from the obtained equality that generalized absorbing BCs cannot guarantee unconditional non increasment of the total mass.

2.3. **Transparent boundary conditions.** The original domain $x \in \mathbf{R}$ is divided into three subdomains $[-\infty,-X]$, $[-X,X]$, $[X,\infty]$, and the initial problem is divided into three subproblems. Transparent BCs (TBC) are obtained by using the assumption that in the exterior domains the solution decreases to zero as $|x| \to \infty$ and the potentials are constant. Then the Dirichlet-to-Neumann maps are defined at the boundaries. Since the potentials are constant, exterior problems can be solved explicitly by the Laplace method (see [12, 17, 9]). We get the following BCs (here we assume that $V \equiv 0$ in the exterior domains):

$$\pm iD_f\frac{\partial u}{\partial x}(\pm X,t) = -i\sqrt{\frac{D_f}{\pi}}e^{i\pi/4}\frac{d}{dt}\int_0^t \frac{u(\pm X,s)}{\sqrt{t-s}}\,ds. \tag{2.16}$$

We note that the nonlocal operator on the right hand side defines a fractional time derivative

$$\sqrt{\frac{d}{dt}}\,v(t) := \frac{1}{\sqrt{\pi}}\frac{d}{dt}\int_0^t \frac{v(s)}{\sqrt{t-s}}\,ds.$$

These derivatives arise in a formal factorization of the Schrödinger equation into left and right travelling waves [9]:

$$\left(\frac{\partial}{\partial x} - \frac{e^{i\pi/4}}{\sqrt{D_f}}\sqrt{\frac{\partial}{\partial t}}\right)\left(\frac{\partial}{\partial x} + \frac{e^{i\pi/4}}{\sqrt{D_f}}\sqrt{\frac{\partial}{\partial t}}\right)u(x,t) = 0.$$

The well-posedness of the initial boundary-value problems in a bounded domain with transparent boundary conditions was investigated also in [18].

The TBCs are non-local in t and they require the storage of the solution on the boundary at all previous time moments. It depends on a problem what strategy is more efficient – to solve numerically the Schrödinger problem in the extended space domain or to use the transparent boundary conditions and to store a solution at the boundary. Our goal is to investigate the accuracy of discrete transparent boundary conditions when the memory length is truncated at some fixed level. This problem is close to application of the fractional Kalman filter for systems of fractional order, arising e.g. in soft matter physics, theory of complex materials and simulations of viscoelastic behavior (see [19] for a description of such problems and application of the fractional Kalman filters).

Following [7], we approximate the nonlocal TBC with a local operator of the form

$$\pm\, i\sqrt{D_f}\frac{\partial u}{\partial x}\big(\pm X,t\big)=\beta u(\pm X,t)+\sum_{k=1}^{m} a_k\big(u(\pm X,t)-d_k\varphi_k^{\pm}(t)\big),\quad m\ge 1, \tag{2.17}$$

$$\frac{d\varphi_k^{\pm}}{dt}=i\left(u(\pm X,t)-d_k\varphi_k^{\pm}(t)\right),\quad t>0;\quad \varphi_k^{\pm}(0)=0.$$

In [7], the well-posedness of the Schrödinger initial-boundary value problem with such approximate TBC is proved and analytic expressions for real nonnegative parameters β, d_k, a_k guarantying the estimate (2.4) at high m are given.

Furthermore, the role of the reflection coefficient is emphasized in [7]. Let assume that we solve the Schrödinger initial-boundary value problem in the time interval $(0,T]$. For small m, the optimal values of coefficients β, a_k and d_k are obtained by minimizing the reflection coefficient in the L^2 norm with the weight $1/\big(1+r^2\big)$

$$\int_0^{T/2\pi}\left|\frac{\sqrt{r}-\beta r-\sum_{k=1}^{m}\big(a_k r/(1+d_k r)\big)}{\sqrt{r}+\beta r+\sum_{k=1}^{m}\big(a_k r/(1+d_k r)\big)}\right|^2\frac{dr}{1+r^2}\longrightarrow \min\,. \tag{2.18}$$

We note, that nonlocal BCs (2.16) are equivalent to the well-known impedance boundary conditions, e.g.:

$$u(X,t)=-\frac{e^{-i\pi/4}}{\sqrt{2\pi}}\int_0^t\frac{\frac{\partial u}{\partial x}(X,t-\tau)\,e^{i\tau}}{\sqrt{\tau}}\,d\tau.$$

Such BCs where applied for the parabolic equation model in underwater acoustics [20] and for the numerical modelling of gyrotrons [21].

3. Finite-Difference Schemes

We introduce a uniform mesh in x on the interval $[-X,X]$: $\bar\omega_h=\{x_j : x_j=-X+jh,\ j=0,\dots,J,\ x_J=X\}$ and a uniform mesh in t on the interval $[0,T]$: $\bar\omega_\tau=\{t^n : t^n=n\tau,\ n=0,\dots,N,\ t^N=T\}$. We also need sub-meshes $\omega_h:=\bar\omega_h/\{x_0,x_J\}$, $\omega_\tau:=\bar\omega_\tau/\{0\}$. Let us define discrete functions $U_j^n=U(x_j,t^n)$, $(x_j,t^n)\in\bar\omega_h\times\bar\omega_\tau$. Then we define the forward and backward difference quotients with respect to x and the backward difference quotient and the symmetric averaging operator in time

$$\partial_x U_j:=\frac{U_{j+1}-U_j}{h},\ \bar\partial_x U_j:=\frac{U_j-U_{j-1}}{h},\ \bar\partial_t U^n:=\frac{U^n-U^{n-1}}{\tau},\ U^{n-1/2}:=\frac{U^n+U^{n-1}}{2}.$$

In this paper we investigate mainly the standard Crank-Nicolson approximation of the Schrödinger equation (2.2):

$$\bar\partial_t U_j^n+iD_f\partial_x\bar\partial_x U_j^{n-1/2}+(\alpha_j-iV_j)U_j^{n-1/2}=0,\quad (x_j,t^n)\in\omega_h\times\omega_\tau. \tag{3.1}$$

The Crank-Nicolson scheme is a very popular tool in solving nonlinear optics problems, since it leads to conservative approximations of nonlinear problems (see, e.g. [16, 2, 22, 23, 3, 24, 25, 26, 27, 28]). Similar schemes were also studied in context of approximate transparent and absorbing BCs [18, 29, 30, 7, 5].

Let us introduce some mesh counterparts of the inner products and the norms in the discrete $L_2(\omega_h)$ and $L_2(\bar{\omega}_h)$ spaces:

$$(U,W)_{\omega_h} = \sum_{j=1}^{J-1} U_j W_j^* h,\ (U,W)_{\bar{\omega}_h} = \sum_{j=1}^{J-1} U_j W_j^* h + \frac{h}{2}\Big(U_0 W_0^* + U_J W_J^*\Big),\ \|U\|_D^2 = (U,U)_D.$$

In the present paper we shall show how for different BCs the presented Crank-Nicolson scheme allows to keep the conservation or dissipation relations for the discrete analogues of mass M_h and energy E_h defined by

$$M_{h,D}^n = \|U^n\|_D^2, \quad E_{h,D}^n = \sum_{j=1}^{J} D_f \big|\bar{\partial}_x U_j^n\big|^2 h + (VU^n, U^n)_D, \quad D = \omega_h, \bar{\omega}_h.$$

3.1. **Discrete reflective boundary conditions.** In this section we approximate the initial-boundary value problem (2.2), (2.3), (2.5) by the following finite-difference scheme

$$\begin{cases} \bar{\partial}_t U_j^n + iD_f \partial_x \bar{\partial}_x U_j^{n-1/2} + (\alpha_j - iV_j) U_j^{n-1/2} = 0, & (x_j, t^n) \in \omega_h \times \omega_\tau, \\ U_0^n = 0, \quad U_J^n = 0, \quad t^n \in \omega_\tau, \\ U_j^0 = u_0(x_j), \quad x_j \in \bar{\omega}_h. \end{cases} \tag{3.2}$$

Now we will prove that the finite difference scheme (3.2) conserves the discrete analogs of mass M_{h,ω_h}^n and energy E_{h,ω_h}^n.

Theorem 3.1 (Discrete analogue of Lemma 2.1)**.** *If $\alpha(x) \geq 0$ and U^n is the solution of finite-difference scheme (3.2), then the discrete total mass of the solution is not increased in time:*

$$M_{h,\omega_h}^n \leq M_{h,\omega_h}^{n-1} \leq \ldots \leq M_{h,\omega_h}^0. \tag{3.3}$$

If $\alpha(x) \equiv 0$ (i.e. the potential function is real valued), then the discrete total mass M_{h,ω_h}^n and energy E_{h,ω_h}^n of (3.2) are conserved:

$$M_{h,\omega_h}^n = M_{h,\omega_h}^{n-1} = \ldots = M_{h,\omega_h}^0, \quad E_{h,\omega_h}^n = E_{h,\omega_h}^{n-1} = \ldots = E_{h,\omega_h}^0. \tag{3.4}$$

Proof. Computing the discrete inner product of finite-difference equation (3.2) with $U^{n-1/2}$, applying the summation by parts of the discrete diffraction operator [15] and using the homogeneous boundary conditions of (3.2), taking the real part of the obtained equality we get the discrete mass conservation equation

$$\|U^n\|_{\omega_h}^2 + 2(\alpha\, U^{n-1/2},\, U^{n-1/2})_{\omega_h} = \|U^{n-1}\|_{\omega_h}^2.$$

Since $\alpha_j \geq 0$, the proof of (3.3) follows trivially. If $\alpha_j \equiv 0$, then we get that the total discrete mass of the solution is conserved, i.e. $M_{h,\omega_h}^n = M_{h,\omega_h}^0$ for any $n \geq 1$.

In order to prove the energy conservation (3.4), we compute the discrete inner product of equation (3.2) with $\bar{\partial}_\tau U^n$, apply the summation by parts of the discrete diffraction operator and take the imaginary part of the the obtained equality:

$$E_{h,\omega_h}^n = E_{h,\omega_h}^{n-1} + 2\sum_{j=1}^{J-1} \alpha_j \operatorname{Im}\Big(U_j^{n-1/2}\, \bar{\partial}_t U_j^{n*}\Big). \tag{3.5}$$

Taking into account the assumption $\alpha \equiv 0$, we get the energy conservation law (3.4). $\square$

The obtained estimates prove the stability of the finite difference scheme (3.2) with respect to the initial condition. Similarly to the analysis given in Section 2 we can prove the discrete analogue of Lemma 2.2 and get estimates of the discrete solution in the maximum norm.

In most cases the Crank-Nicolson scheme gives a stable approximation of nonlinear Schrödinger equations. But for a damped nonlinear Schrödinger equation the application of the Crank-Nicolson scheme can lead to a non stable discrete problem if the balance of the damping force and mass compensation is approximated in non conservative way (see, [31]).

In order to see numerical effects of the reflecting BCs we solve the initial-boundary value problem (2.2), (2.3), (2.5) for $V(x) \equiv 0$, $D_f = 1$, setting first $\alpha(x) \equiv 0$. We take a standard example of the Gaussian solution

$$u(x,t) = \frac{1}{\sqrt{1 - it/w_0}} \exp\left[-ik(x-kt) - \frac{(x-2kt)^2}{4(w_0 - it)}\right]. \tag{3.6}$$

This example is chosen in many papers on numerical approximations of absorbing and transparent BCs. We take the following values of parameters: $w_0 = 0.15$, $k = 2$, the domain of interest is defined as $[-2, 2]$, i.e. $\tilde{X} = 2$. At the initial $t = 0$ solution $|u(x,0)|^2 = |u_0(x)|^2 = e^{-x^2/2\omega_0}$, i.e., the initial data are mainly confined within the interval $|x| < 3\sqrt{\omega_0}$. Both effects, the diffraction and linear transport with the wave number k, are important in this example.

The absolute values of the exact solution are changing monotonically in time and space (while the real and imaginary parts of the solution are rapidly oscillating). This property is very important in solving nonlinear problems when even small numerical oscillations can grow up significantly due to the nonlinear interaction. Thus our prime goal is to reduce the reflections from boundaries introduced by artificial boundary conditions (2.5).

In many papers (see [32, 4]) it is proposed to compare the properties of discrete artificial BCs in terms of reflection. The reflection ratio at time t^n is calculated as

$$r^n = \frac{\sum_{j=s}^{f} |U_j^n|^2}{\sum_{j=s}^{f} |U_j^0|^2}, \quad x_s = -\tilde{X}, \ \ x_f = \tilde{X},$$

i.e. a summation is done over the domain of interest.

We compute solutions of the finite-difference scheme (3.2) for $0 \le t \le 1$ with different lengths X of the extended domain. Fig. 1a shows plots of reflection ratio as a function of time for the exact Gaussian solution (3.6) and for the numerical solutions simulated in restricted computational domains.

For all computations the time and space mesh steps are selected sufficiently small in order not to influence the presented results.

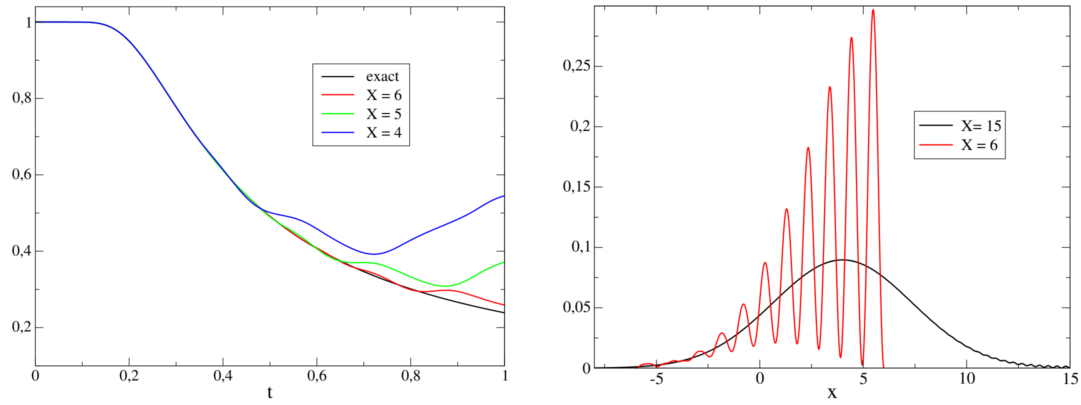

a) b)

FIGURE 1. Numerical results for finite difference scheme (3.2): a) the reflection ratio a function of time for the exact Gaussian solution (3.6) and for the numerical solutions simulated in restricted computational domains, b) plots of $|U^n|$ at $t = 1$ for extended domains with $X = 6$ and $X = 15$.

At the beginning the traveling wave is located in the interior of the domain of interest, thus the reflection ratio as a function of time remains constant. Later, the exact wave smoothly passes through the boundary and the reflection ratio continuously decreases as a function of time. The presented results show that for a satisfactory approximation of the reflection ratio of the exact solution (3.6) at higher t one needs to increase the size X of the extended domain.

Generally, the waves reflected from the boundary return back to the computational domain and disturb the solution. Even in the case of the large artificial domain with $X = 6$ the obtained reflected solution is highly oscillating (see, Fig. 1b, where numerical solutions computed in a truncated domains with $X = 6, 15$ are plotted at $t = 1$). Only in the case of $X = 15$ the numerical solution approximates very well the exact solution (3.6). These oscillations prove that a good approximation of the reflection ratio is not sufficient indicator of the accuracy in the maximum norm, since it defines an averaged characteristic of the solution. As a conclusion, we note that such simple reflective artificial BCs cannot be recommended for simulations of nonlinear interactions of laser waves in real world applications, since the nonlinearities are defined pointwise, not in averaged sense.

In order to damp parasitic waves reflected from the boundary we formulate near the boundary an absorbing layer with the absorbing coefficient α_0. Let us consider the extended domain with $X = 3$ and take the following absorbing layer $\alpha(x) = 0$, if $|x| \leq 2.5$ and $\alpha(x) = \alpha_0$ otherwise. We have computed the solution of the finite-difference scheme (3.2) for $0 \leq t \leq 0.5$ with different values of the absorption coefficient α_0 and have determined the optimal value of α_0, when oscillations of the reflected waves are reduced in most effective way. In Fig. 2a we present the modulus of the exact solution and the numerical solutions computed in a truncated domain without absorption layer and with the optimal value $\alpha_0 = 10$. The oscillations are reduced essentially when the absorbing layer is optimized.

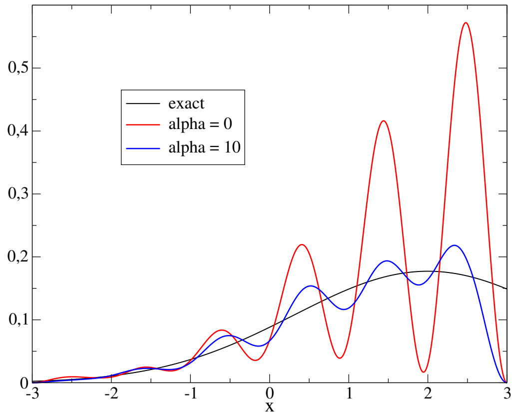

a)

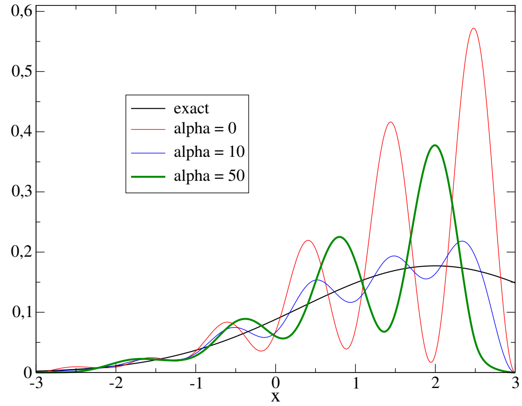

b)

FIGURE 2. Numerical results for finite difference scheme (3.2) in the extended domain with $X = 3$ and various values of the absorption coefficient: a) plots of $|U^n|$ for the solution (3.6) and for the numerical solutions with $\alpha_0 = 0, 10$, b) plots of $|U^n|$ for the numerical solutions with $\alpha_0 = 0, 10, 50$.

If we try further to increase the value of α_0, then reflective boundaries are produced at $\hat{X} = X - \Delta x_l$ and amplitudes of oscillations again start to increase. Such a situation is illustrated in Fig. 2b, where the numerical solution is presented for $\alpha_0 = 50$.

In many problems of optics and optoelectronics, however, we have a nonvanishing potential V which can prevent or accelerate the diffractive spreading of the optical field. In the following example we set again the damping function $\alpha \equiv 0$, $X = 4$, assume the potential $V(x) = 50$, $|x| \geq X_\delta = 2$, and $V(x) = 0$ for $|x| < X_\delta$ and compute the solution of the finite difference scheme (3.2) starting with initial function u_0 defined by (3.6). Fig. 3a plots the modulus of the numerical solutions $|U^n|$ for three different time moments $t = 0.2, 0.4, 0.8$. In Fig. 3b we present the plot of computed reflection ratio as a function of time in the domain $[-X_\delta, X_\delta]$. It is clear that the traveling wave is localized in the domain of interest during the whole integration time and only a small part of the mass has moved outside of this domain. Since the maximal norm of the numerical solution is bounded, the oscillations of the numerical solution do not increase in time.

In the case of the inverse potential with $V(x) = -50$ for $|x| \geq X_\delta$ instead of a localization of the numerical solution we can observe the acceleration of the field spreading out of computational domain. Results of computations are presented in Fig. 4.

3.2. **Absorbing boundary conditions.** In this section we approximate the initial-boundary value problem (2.2), (2.3) with absorbing boundary conditions (2.11) by

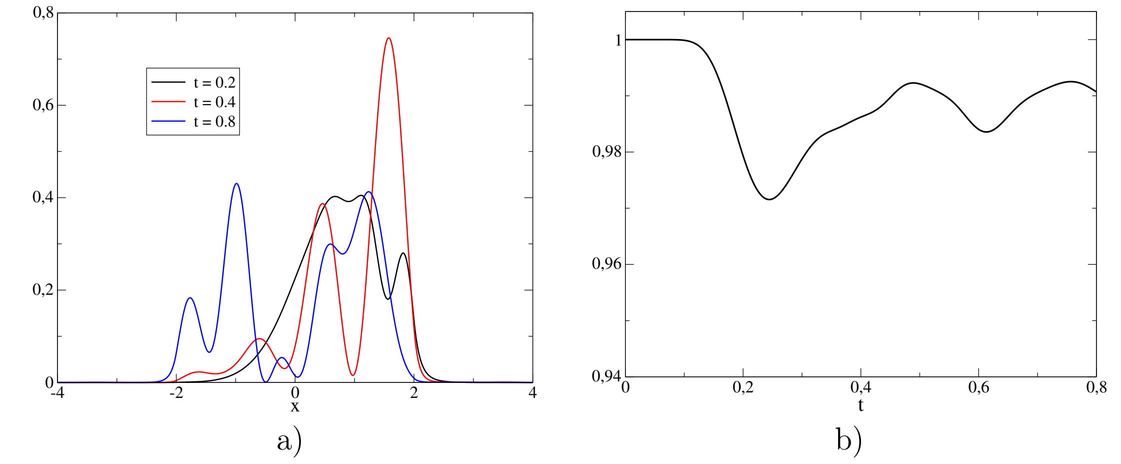

FIGURE 3. Solutions of the finite difference scheme (3.2) with $V = 50$ at various time moments: a) plots of $|U^n|$ for $t = 0.2, 0.4, 0.8$, b) reflection ratio as a function of time.

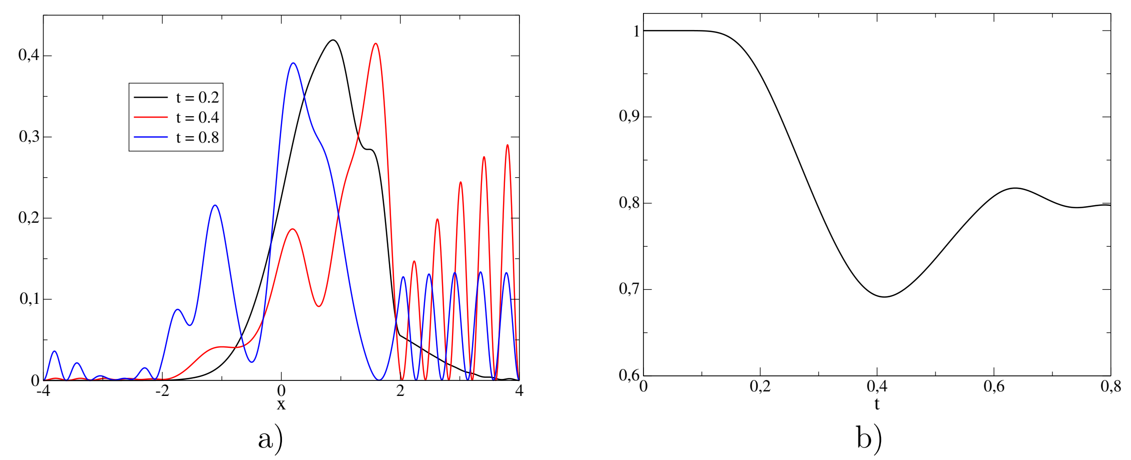

FIGURE 4. Solutions of the finite difference scheme (3.2) with a negative potential $V = -50$ for $|x| \geq X_\delta$ at various time moments: a) plots of $|U^n|$ for $t = 0.2, 0.4, 0.8$, b) reflection ratio as a function of time.

the following finite-difference scheme

$$\begin{cases} \bar{\partial}_t U_j^n + iD_f \partial_x \bar{\partial}_x U_j^{n-1/2} - iV_j U_j^{n-1/2} = 0, \quad (x_j, t^n) \in \omega_h \times \omega_\tau, \\ -iD_f \partial_x U_0^{n-1/2} - \dfrac{h}{2}\left(\bar{\partial}_t U_0^n - iV_0 U_0^{n-1/2}\right) = \gamma U_0^{n-1/2}, \quad t^n \in \omega_\tau, \\ iD_f \bar{\partial}_x U_J^{n-1/2} - \dfrac{h}{2}\left(\bar{\partial}_t U_J^n - iV_J U_J^{n-1/2}\right) = \gamma U_J^{n-1/2}, \\ U_j^0 = u_0(x_j), \quad x_j \in \bar{\omega}_h. \end{cases} \tag{3.7}$$

Theorem 3.2 (Discrete analogue of Lemma 2.3)**.** *Let U^n be the solution of finite-difference scheme (3.7), then the discrete total mass of the numerical solution $M^n_{h,\bar{\omega}_h}$*

is not increased in time:

$$M^n_{h,\bar\omega_h} \le M^{n-1}_{h,\bar\omega_h} \le \ldots \le M^0_{h,\bar\omega_h}. \tag{3.8}$$

The discrete energy $E^n_{h,\bar\omega_h}$ of the numerical solution satisfies the following conservation equation

$$E^n_{h,\bar\omega_h} - E^{n-1}_{h,\bar\omega_h} = 2\gamma\tau \left(\operatorname{Im} U_0^{n-1/2} \big(\bar\partial_t U_0^n\big)^* + \operatorname{Im} U_J^{n-1/2} \big(\bar\partial_t U_J^n\big)^* \right). \tag{3.9}$$

Proof. Computing the discrete inner product of finite-difference equation (3.2) with $U^{n-1/2}$, applying the summation by parts of the discrete diffraction operator [15] we get the equality

$$(\bar\partial_t U^n, U^{n-1/2})_{\omega_h} - iD_f \sum_{j=1}^{J} \big|\bar\partial_x U_j^{n-1/2}\big|^2 h + iD_f \bar\partial_x U_J^{n-1/2} \big(U_J^{n-1/2}\big)^*$$
$$- iD_f \partial_x U_0^{n-1/2} \big(U_0^{n-1/2}\big)^* - i(VU^{n-1/2}, U^{n-1/2})_{\omega_h} = 0.$$

Using the absorbing boundary conditions (3.2), we have

$$(\bar\partial_t U^n, U^{n-1/2})_{\bar\omega_h} - iD_f \sum_{j=1}^{J} \big|\bar\partial_x U_j^{n-1/2}\big|^2 h - i(VU^{n-1/2}, U^{n-1/2})_{\bar\omega_h}$$
$$+ \gamma \left(|U_J^{n-1/2}|^2 + |U_0^{n-1/2}|^2 \right) = 0.$$

Taking the real part of the obtained equality we get the discrete mass conservation equation

$$\|U^n\|^2_{\bar\omega_h} + 2\tau\gamma \left(|U_0^{n-1/2}|^2 + |U_J^{n-1/2}|^2 \right) = \|U^{n-1}\|^2_{\bar\omega_h}.$$

Since $\gamma \ge 0$, the proof of (3.8) follows trivially.

In order to prove (3.9) we compute the discrete inner product of finite-difference equation (3.2) with $\bar\partial_t U^n$, apply the summation by parts of the discrete diffraction operator:

$$\big\|\bar\partial_t U^n\big\|^2_{\omega_h} - iD_f \sum_{j=1}^{J} \bar\partial_x U_j^{n-1/2} \left(\bar\partial_t \bar\partial_x U_j^n\right)^* h + iD_f \bar\partial_x U_J^{n-1/2} \big(\bar\partial_t U_J^n\big)^*$$
$$- iD_f \partial_x U_0^{n-1/2} \big(\bar\partial_t U_0^n\big)^* - i(VU^{n-1/2}, \bar\partial_t U^n)_{\omega_h} = 0.$$

Using the absorbing boundary conditions, we have

$$\big\|\bar\partial_t U^n\big\|^2_{\bar\omega_h} - iD_f \sum_{j=1}^{J} \bar\partial_x U_j^{n-1/2} \left(\bar\partial_t \bar\partial_x U_j^n\right)^* h - i(VU^{n-1/2}, \bar\partial_t U^n)_{\bar\omega_h}$$
$$+ \gamma \left(U_0^{n-1/2} \big(\bar\partial_t U_0^n\big)^* U_J^{n-1/2} \big(\bar\partial_t U_J^n\big)^* \right) = 0.$$

Taking the imaginary part of the obtained equality we prove (3.9). □

We compute the solution of the finite-difference scheme (3.7) with potential $V \equiv 0$, initial $u_0(x)$ determined by (3.6) for $0 \le t \le 1$ and different values of the parameter $\gamma = 2.5, 5, 8, 10$. The computational domain is fixed to the interval $[-2.5, 2.5]$. Fig. 5b shows plots of the reflection ratio as a function of time for the exact solution

(3.6) and for the numerical solutions computed with $\gamma = 5, 10$. In Fig. 5a the modulus of the exact and numerical solutions are presented at $t = 0.5$.

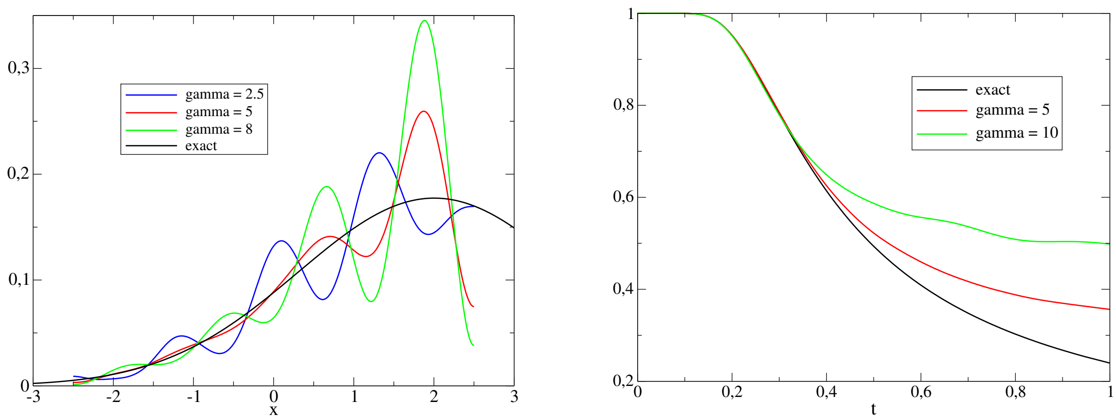

a) b)

FIGURE 5. Numerical solutions of the finite difference scheme (3.7) with $\gamma = 2.5, 5, 10$: a) plots of $|U^n|^2$ at $t = 0.5$, b) the reflection ratio as a function of time.

Fig. 5 shows that precision of the numerical solution depends strongly on the selection of γ. Note, that in the present case the best approximation is achieved for $\gamma = 2.5$ which is close to the half of the group velocity of the exact solution at $X = 2.5$ and $t = 0.5$. It seems also that absorbing BCs are more robust than simple reflective BCs.

3.3. **Transparent boundary conditions.** The main difficulty of the numerical approximation of nonlocal TBCs (2.16) is linked to the presence of a convolution operator in the BCs. Some straightforward discretizations of TBCs destroys the unconditional stability of the basic Crank-Nicolson scheme or induce numerical reflection at the boundaries and therefore reduce the accuracy of the Crank-Nicolson scheme achieved in the whole-space domain (see [18, 8, 9] for a review on different discrete approximations of nonlocal TBCs).

Stable finite difference schemes for numerical approximation of the Schrödinger problem with the nonlocal TBCs are proposed in [18, 30, 9]. They use the standard Crank-Nicolson scheme inside of the computational domain and introduce special discretizations of the BC. In [30] a class of finite difference schemes is proposed, they include various generalizations of the Crank-Nicolson scheme derived by the finite difference, finite volume and finite element methods.

Following [9], we consider the exact discrete transparent BC (DTBC) for the Crank-Nicolson finite difference discretization, such that the numerical solution in the reduced domain is the same as for the whole-space problem. The derivation of the discrete TBC mimics the derivation of the analytic TBC (2.16) on a discrete level.

The DTBCs are defined as follows:

$$U_1^n = \sum_{k=1}^{n} U_0^k l_0^{n-k} - U_1^{n-1}, \quad U_{J-1}^n = \sum_{k=1}^{n} U_J^k l_J^{n-k} - U_{J-1}^{n-1}, \tag{3.10}$$

with

$$l_j^k = \left(1 + i\frac{R}{2} + \frac{\sigma_j}{2}\right)\delta_k^0 + \left(1 - i\frac{R}{2} + \frac{\sigma_j}{2}\right)\delta_k^1 + \beta_j e^{ik\varphi_j}\frac{P_k(\mu_j) - P_{k-2}(\mu_j)}{2k-1},$$

$$\varphi_j = \arctan\frac{2R(\sigma_j+2)}{R^2 - 4\sigma_j - \sigma_j^2}, \quad \mu_j = \frac{R^2 + 4\sigma_j + \sigma_j^2}{\sqrt{(R^2+\sigma_j^2)\left(R^2 + (\sigma_j+4)^2\right)}},$$

$$\sigma_j = \frac{h^2}{D_f}V_j, \quad R = \frac{2h^2}{D_f\tau}, \quad \beta_j = -\frac{i}{2}\left[(R^2+\sigma_j^2)\left(R^2+(\sigma_j+4)^2\right)\right]^{1/4} e^{-i\varphi_j/2}, \quad j = 0, J.$$

Here P_k denotes the Legendre polynomials ($P_{-1} \equiv 0$, $P_{-1} \equiv 0$) and δ_n^j is the Kronecker symbol.

The implementation of the Crank-Nicolson finite difference scheme with the discrete TBC (3.10) requires to store the numerical solution U_j^k on boundary points $j = 0, J$ for all time levels (due to a nonlocal approximation of the convolution operator the boundary data from the whole past history is used). In order to reduce the memory requirements we will consider the accuracy of this algorithm, when the length of the saved data is fixed to m time steps. Figure 6a shows the modulus of the numerical solutions of (3.1), (3.10) at $t = 0.5$ with $V \equiv 0$, $X = 2.5$ for the full DTBC and the truncated version of DTBC(m).

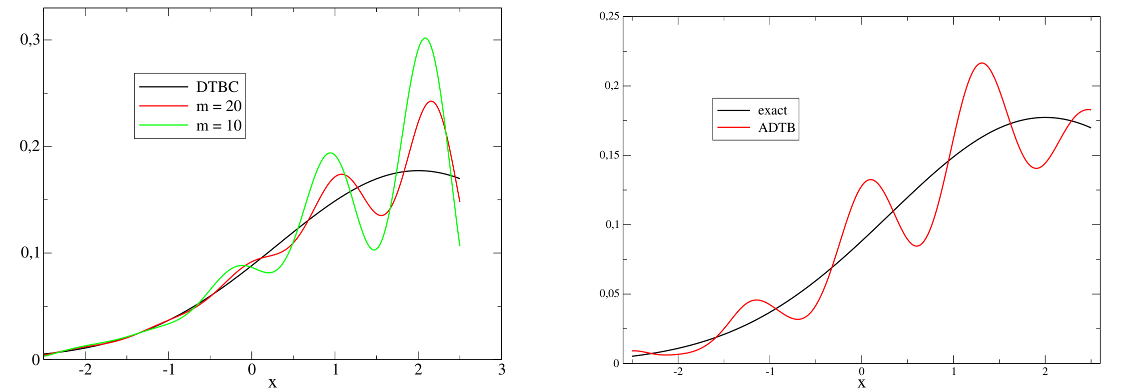

a) b)

FIGURE 6. Numerical solutions of the scheme (3.1) with $V \equiv 0$ for a) the DTBC (3.10) and the truncated version of DTBC(m), and for b) the approximate DTBC (3.11).

We see that a simple truncation of coefficients l_j^k in DTBC (3.10) induces strong numerical reflections. Computational experiments show that these oscillations scale as N/m, thus if the accuracy of approximation requires a smaller time step, then the truncation parameter m should be enlarged accordingly.

Next let us consider the Schrödinger problem with the BC (2.17), which approximates TBC by using rational functions. The discrete version of this condition is obtained by applying the finite volume method (here we consider the boundary equation at $x = X$):

$$
\begin{aligned}
(3.11)\qquad & i\sqrt{D_f}\bar{\partial}_x U_J^{n-1/2} - \frac{h}{2\sqrt{D_f}}\left(\bar{\partial}_t U_J^n - iV_J U_J^{n-1/2}\right) = \beta U_J^{n-1/2} \\
& \qquad + \sum_{k=1}^{m} a_k \left(U_J^{n-1/2} - d_k \Phi_k^{n-1/2}\right),
\end{aligned}
$$

$$
(3.12)\qquad \bar{\partial}_t \Phi_k^n + i\left(d_k \Phi_k^{n-1/2} - U_J^{n-1/2}\right) = 0, \quad \Phi_k^0 = 0, \quad k = 1, \ldots, m.
$$

In [7] a similar finite difference approximation is obtained by using the ghost points at the boundaries and approximating the fluxes by the central difference formula.

At each time level a solution of (3.11) – (3.12) is computed by the following algorithm. First, by using the equality $\Phi_k^{n-1/2} = \Phi_k^{n-1} + \frac{\tau}{2}\bar{\partial}_t \Phi_k^n$ we obtain from (3.12) that

$$
\Phi_k^{n-1/2} = \frac{1}{1 + i\tau d_k/2}\left(\Phi_k^{n-1} + i\frac{\tau}{2}U_J^{n-1/2}\right).
$$

Substituting it into (3.11) and using the Crank-Nicolson scheme for interior points of the grid $j = 1, \ldots, J-1$, we get a system with a tridiagonal matrix for vector $U^{n-1/2}$. Such systems are solved efficiently by using the factorization algorithm.

Figure 6b shows the results obtained in the case $m = 1$. The coefficients of the approximate DTBC are obtained in [7] with the simplex method: $\beta = 0.7269284$, $a_1 = 2.142767$, $d_1 = 6.906263$.

4. Conclusions

In this paper we consider finite difference approximations of a 1-dimensional linear Schrödinger equation with three different types of artificial BCs. These boundary conditions allow to compute numerically the solution of the problem given on an infinite domain. For reflecting and absorbing BC we have proved that the discrete solution satisfies conservation laws for the mass and the energy if such integrals are conserved for the differential problem.

Results of computational experiments show that the reflective boundary conditions can be applied only if artificial BCs are formulated for a sufficiently large domain and, therefore, they cannot be used for many real world applications. The absorbing BCs are efficient if the solution consists of only few simple waves, but, in general, they can be more efficient than the reflective BCs. A similar effect is achieved by using the artificial layer at the boundaries of the domain with a potential $i\alpha(x)$ (we get a sink term).

Most promising are DTBC(m), where the length of memory is restricted to m time steps and m is defined in consistent way with the discrete time step τ. Another interesting possibility is to approximate nonlocal in time TBCs by using the rational local approximations.

Acknowledgment. This work was supported by the Lithuanian State Science and Studies Foundation within the project B-03/2007 and by the Agency for International Science and Technology Development Programmes in Lithuania within the EUREKA project E!3691 OPTCABLES. The work of M. Radziunas has been supported by DFG Research Center MATHEON

References

[1] J.J. Lim, T.M. Benson, and E.C. Larkins. Design of wide-emitter single-mode laser diodes. *IEEE J. Quantum Electron.*, 41:506–516, 2005.

[2] R. Čiegis, M. Radziunas, and M. Lichtner. Numerical algorithms for simulation of multisection lasers by using traveling wave model. *Mathematical Modelling and Analysis*, 13(3):327–348, 2008.

[3] I. Laukaitytė, R. Čiegis, M. Lichtner, and M. Radziunas. Parallel numerical algorithm for the traveling wave model. In R. Ciegis, D. Henty, B. Kagstrōm, and J. Žilinskas, editors, *Parallel Linear Algebra and Optimization: Advances and Applications. Springer Optimization and Its Applications. ISBN: 978-0-387-09706-0*, volume 27, pages 237–250, New-York, 2009. Springer.

[4] T. Fevens and H. Jiang. Absorbing boundary conditions for the Schrödinger equation. *SIAM J. Sci. Comput.*, 21(1):255–282, 1999.

[5] Chen Zhidong, Zhang Jinyu, and Yu Zhiping. Solution of the time-dependent Schrödinger equation with absorbing boundary conditions. *Journal of Semiconductors*, 30(1):1–6, 2009.

[6] D. Givoli and B. Neta. High-order non-reflecting boundary scheme for time-dependent waves. *J. Comput. Phys.*, 186(1):24–44, 2003.

[7] J. Szeftel. Design of absorbing boundary conditions for Schrödinger equation in R^d. *SIAM J. Numer. Anal.*, 42(4):1527–1551, 2004.

[8] V.A. Baskakov and A.V. Popov. Implementation of transparent boundaries for numerical solution of the Schrödinger equation. *Wave Motion*, 14(1):123–128, 1991.

[9] M. Ehrhardt. Discrete transparent boundary conditions for general Schrödinger – type equations. *VLSL Design*, 9(4):325–338, 1999.

[10] A. Arnold and M. Ehrhardt. Discrete transparent boundary conditions for wide angle parabolic equations in underwater acoustics. *J. Comp. Phys.*, 145:611–638, 1998.

[11] J. Jr. Douglas, J.E. Santos, D. Sheen, and L.S. Bennethum. Frequency domain treatment of one-dimensional scalar waves. *Math. Mod. and Meth. in Appl. Sc.*, 3:171–194, 1993.

[12] X. Antoine, A. Arnold, C. Besse, M. Ehrhardt, and A. Schadle. A review on transparent and artificial boundary conditions technique for linear and nonlinear Schrödinger equations. *Commun. Comput. Phys.*, 4(4):729–796, 2008.

[13] R. Kosloff and D. Kosloff. Absorbing boundary conditions for wave propagation problems. *J. Comput. Phys.*, 63(2):363–376, 1986.

[14] S. Larsson and V. Thomee. *Partial Differential Equations with Numerical Methods. Texts in Applied Mathematics*. Springer, 2003.

[15] A.A. Samarskii. *The theory of difference schemes*. Marcel Dekker, Inc., New York–Basel, 2001.

[16] R. Čiegis. On the convergence in C norm of symmetric difference schemes for nonlinear evolution problems. *Lith. Math. Journal*, 32(2):187–205, 1992.

[17] A. Arnold, M. Ehrhardt, and I. Sofronov. Discrete transparent boundary conditions for the Schrödinger equation: Fast calculation, approximation, and stability. *Comm. Math. Sci.*, 1:501–556, 2003.

[18] X. Antoine and C. Besse. Unconditionally stable discretization schemes of non-reflecting boundary conditions for the one-dimensional Schrödinger equation. *J. Comp. Phys.*, 188:157–175, 2003.

[19] M. Romanovas, L. Klingbeil, M. Traechtler, and Y. Manoli. Application of fractional sensor fusion algorithms for inertial mems sensing. *Mathematical Modelling and Analysis*, 14(2):199–209, 2009.

[20] J.S. Papadakis, M. Taroudakis, P. Papadakis, and B. Mayfield. A new method for a realistic treatment of the sea bottom in the parabolic approximation. *J. Acoust. Soc. Am.*, 92:2030–2038, 1992.

[21] J. Cepītis, H. Kalis, and A. Reinfelds. Numerical investigations of single mode gyrotron equation. *Mathematical Modelling and Analysis*, 14(2):169–178, 2009.

[22] M. Delfour, M. Fortin, and G. Payre. Finite-difference solution of non-linear Schrödinger equation. *Comp. Math. Phys.*, 44(2):277–288, 1981.

[23] A. Jakušev, R. Čiegis, I. Laukaitytė, and V. Trofimov. Parallelization of linear algebra algoritms using parsol library of mathematical objects. In R. Ciegis, D. Henty, B. Kagstrōm, and J. Žilinskas, editors, *Parallel Linear Algebra and Optimization: Advances and Applications. Springer Optimization and Its Applications. ISBN: 978-0-387-09706-0*, volume 27, pages 25–36, New-York, 2009. Springer.

[24] J. M. Sanz-Serna and J. G. Verwer. Conservative and non-conservative schemes for the solution of the nonlinear Schrödinger equation. *IMA J. Numer. Anal.*, 6(1):25–42, 1986.

[25] T.R. Taha and M.J. Ablovitz. Analytical and numerical aspects of certain nonlinear evolution equations. II. Numerical Schrödinger equation. *J. Comp. Phys.*, 55:203–230, 1994.

[26] V.A. Trofimov and N.V. Peskov. Comparison of finite-difference schemes for the Gross-Pitaevskii equation. *Mathematical Modelling and Analysis*, 14(1):109–126, 2009.

[27] J. A. Weideman and B. M. Herbst. Split-step methods for the solution of the nonlinear Schrödinger equation. *SIAM J. Numer. Anal.*, 23(3):485–507, 1986.

[28] F. Zhang, V.M. Perez-Garcia, and L. Vazquez. Numerical simulation of nonlinear Schrödinger equation: A new conservative scheme. *Appl. Math. Comput.*, 71(2–3):165–177, 1995.

[29] B. Ducomet and A. Zlotnik. On stability of the Crank-Nicolson scheme with approximate transparent boundary conditions for the Schrödinger equation. II. *Comm. Math. Sci.*, 5:267–298, 2007.

[30] B. Ducomet, A. Zlotnik, and I. Zlotnik. On a family of finite-difference schemes with approximate transparent boundary conditions for a generalized 1D Schrödinger equation. *Kinetic and Related Models*, 2(1):151–179, 2009.

[31] R. Čiegis and V. Pakalnytė. The finite difference scheme for the solution of weakly damped nonlinear Schrödinger equation. *Intl. Journal of Applied Science and Computations*, 8(3):127–134, 2001.

[32] I. Alonso-Mallo and N. Reguera. Weak ill-posedness of spatial discretizations of absorbing boundary conditions for Schrödinger type equations. *SIAM J. Numer. Anal.*, 40(1):134–158, 2002.